BOREAL ENVIRONMENT RESEARCH 18: 145–163
ISSN 1239-6095 (print) ISSN 1797-2469 (online)

Helsinki 5 April 2013

# Airborne measurements over the boreal forest of southern Finland during new particle formation events in 2009 and 2010

Siegfried Schobesberger[1)], Riikka Väänänen[1)], Katri Leino[1)], Aki Virkkula[1)], John Backman[1)], Toivo Pohja[1)], Erkki Siivola[1)], Alessandro Franchin[1)], Jyri Mikkilä[1)2)], Mikhail Paramonov[1)], Pasi P. Aalto[1)], Radovan Krejci[1)3)], Tuukka Petäjä[1)] and Markku Kulmala[1)]

[1)] *Division of Atmospheric Sciences, Department of Physics, P.O. Box 64, FI-00014 University of Helsinki, Finland*
[2)] *Airmodus Ltd., Finland, Gustaf Hällströmin katu 2 A, FI-00560 Helsinki, Finland*
[3)] *Department of Applied Environmental Science (ITM), Stockholm University, SE-106 91 Stockholm, Sweden*

*Received 31 Jan. 2012, final version received 30 July 2012, accepted 29 May 2012*

Schobesberger, S., Väänänen, R., Leino, K., Virkkula, A., Backman, J., Pohja, T., Siivola, E., Franchin, A., Mikkilä, J., Paramonov, M., Aalto, P.P., Krejci, R., Petäjä, T. & Kulmala, M. 2013: Airborne measurements over the boreal forest of southern Finland during new particle formation events in 2009 and 2010. *Boreal Env. Res.* 18: 145–163.

We conducted airborne observations of aerosol physical properties over the southern Finland boreal forest environment. The aim was to investigate the lower tropospheric aerosol (up to 4-km altitude) over an area of 250 by 200 km, in particular during new particle formation (NPF) events, and to address the spatial variability of aerosol number concentration and number size distribution. The regional NPF events, detected both airborne and at the ground, with air masses originating from the Arctic or northern Atlantic Ocean were studied throughout the boundary layer and throughout the area covered. Three suitable case studies are presented in more detail. In two of these studies, the concentrations of nucleation mode particles (3–10 nm in diameter) were found considerably higher (up to a factor of 30) in the upper parts of the planetary boundary layer compared to ground-based measurements during the nucleation events. The observed vertical variation can be connected to boundary layer dynamics and interactions between the boundary layer and the lower free troposphere, likely yielding high concentrations of newly formed aerosol particles. Our results suggest that nucleation does not necessarily occur close to the surface. In one presented case we found evidence of NPF occurring in a limited area above cloud, in the complete absence of a regional NPF event.

## Introduction

In the Earth's atmosphere, particulate matter suspended in the air (aerosol particles) is of great significance for the climate and air quality (Forster *et al*. 2007, Arneth *et al*. 2009). The particles act as cloud condensation nuclei (CCN), i.e. seeds for cloud droplets, and have negative impacts on human health (Nel *et al*. 2006, Vaclavik Bräuner *et al*. 2007, Brook *et al*. 2010). Both anthropogenic and natural sources influence the concentration and composition of atmospheric

*Editor in charge of this article: Hannele Korhonen*

aerosol capable of acting as CCN (Weber *et al*. 2003, Clarke and Kapustin 2010, Hamburger *et al*. 2011, Heald *et al*. 2011, Yue *et al*. 2011). The formation of new aerosol particles from gaseous precursors may currently account for about half of all the CCN globally (Merikanto *et al*. 2009) and has been observed in many locations around the world (Kulmala *et al*. 2004, Kulmala and Kerminen 2008).

The spatial extent of new particle formation (NPF) can be inferred indirectly from a single ground-based measurement location (Mäkelä *et al*. 1997, Kulmala *et al*. 2001). If the NPF was only intermittent in nature, the formation and subsequent growth would not be observed continuously at a fixed site. The regional nature of the NPF events has also been observed elsewhere (Stanier *et al*. 2004, Vana *et al*. 2004, Komppula *et al*. 2005, Wehner *et al*. 2007, Hussein *et al*. 2009, Pryor *et al*. 2010). Aerosol measurements onboard an aircraft (Baumgardner *et al*. 2011) can add relevant information also on vertical extent of the NPF (Buzorius *et al*. 2004, Crumeyrolle *et al*. 2010, Mirme *et al*. 2010).

The "European Integrated project on Aerosol Cloud Climate and Air Quality Interactions" (EUCAARI) project was a major effort to study aerosol properties and formation at different locations around Europe to shape a comprehensive view of spatial and temporal variability of the secondary aerosol formation on a continental scale (Kerminen *et al*. 2010, Kulmala *et al*. 2011). During May 2008, airborne measurements were performed as a part of EUCAARI with several research airplanes. The airborne and ground-based measurements of aerosol number concentrations in the accumulation mode were in a good agreement (Hamburger *et al*. 2011). Concerning the ultra-fine particles, the data obtained with the French SAFIRE ATR 42 aircraft around the Cabauw measurement station in the Netherlands indicated that new particle formation occurred with spatial scales of 100 km both over the continental areas as well as over the North Sea (Crumeyrolle *et al*. 2010). Other measurement flights found indication and evidence for nucleation taking place also in the free troposphere (Clarke 1992, Schröder and Ström 1997, Mirme *et al*. 2010).

Airborne aerosol measurements over the boreal environment and focused on the lower troposphere are scarce. The extent of aerosol formation was studied onboard a DHC-6 Twin Otter on three days in March 2003 (O'Dowd *et al*. 2007, 2009) and using a motorized hang glider/microlight aircraft from IMK-IFU (Junkermann 2001, 2005). The formation of new particles was observed throughout the boundary layer over Hyytiälä, while no new particle formation was observed over the frozen sea upwind from Hyytiälä (O'Dowd *et al*. 2009). The onset of new particle formation was observed to coincide with the break of the nocturnal boundary layer, with the process of formation occurring at the ground level from where the fresh new particles were mixed upwards (O'Dowd *et al*. 2009). The aerosol and ion characterization in a hot-air balloon around the Hyytiälä SMEAR-II research station (Hari and Kulmala 2005) indicated that the new particle formation occurred either throughout the mixed layer or close to the surface (Laakso *et al*. 2007). On one out of eleven measurement days with the balloon, the new particle formation was also observed to take place in the free troposphere (Laakso *et al*. 2007). Vertical profiling with a Condensation Particle Counter and an Optical Particle Sizer using a tethered balloon revealed new particle formation homogeneously occurring in the boundary layer over Hyytiälä (Boy *et al*. 2004). In summary, several studies using limited number of observations delivered various results and conclusions instead of a consistent picture. There is a clear need for more experiments, addressing the NPF, to lead towards a better understanding as for where in the planetary boundary layer, and under what conditions, new aerosol particles are formed.

The study presented here was a part of the EUCAARI project and aims at examining both the vertical and the horizontal extent of new particle formation in the boreal forest environment, based on aircraft measurements. We present a compact aircraft platform for aerosol measurements, which has relatively inexpensive running costs. These airborne measurements are compared with the ground-based measurements conducted at the well-equipped SMEAR II (Station for Measuring Forest Ecosystem–Atmosphere

**Fig. 1**. Photographs of the inlet mounted on the right wing of the measurement aircraft.

Relations II) station, located in Hyytiälä in the boreal forest of southern Finland.

## Experimental setup and methods

### Aircraft and inlets

Results presented here are based on the data collected by an airborne measurement platform and these data are related to ground based observations. The aircraft used was a Cessna FR172F, a light single-engine airplane. This particular airplane was modified to accommodate the measurement equipment. The majority of the instruments was built into a rack behind the front-row seats, and was supplied with sample air collected from an external inlet mounted on the airplane's right wing facing the undisturbed air ahead (Fig. 1). The aerosol inlet's design was adopted from the University of Hawai'i shrouded solid diffuser inlet design originally presented in McNaughton *et al*. (2007) for use aboard a DC-8 aircraft. Our inlet is a downsized version of it, suiting the lower cruising speed of the Cessna. The sample air was transported to the instruments in the aircraft's cabin through stainless steel tubing (22 mm inner diameter, Figs. 1 and 2), running from the inlet back under the wing and along the wing strut towards the cabin where it entered from underneath. The total length of the sample line is between 3.8 and 4.3 m, depending on the exact position of the respective instrument in the rack. Excess sample air not used by the instruments exited through a venturi (mounted on the right main gear leg, Figs. 1 and 2). The forward movement of the flying airplane together with the suction in the venturi provided the necessary sample air flow. It was controlled manually using a flow meter (TSI 4000 series) and a manual valve, to maintain a constant sampling flow of 50 l $min^{-1}$.

A typical measurement flight consisted of four vertical profiles flown with an airspeed of 125 km $h^{-1}$ and a climb/descent rate of 150 m $min^{-1}$ from altitudes of 300 m up to 4000 m. As compared with many earlier flight measurements (e.g. Mirme *et al*. 2010), the airspeed, scale of altitudes, and areas covered by our measurements was smaller, thus allowing for a higher spatial and temporal resolution.

### Airborne instrumentation

The following instrumentation was implemented for observations discussed in this study (Fig. 2): a $CO_2/H_2O$ analyzer (LI-COR LI-840), a TSI 3776 condensation particle counter (CPC) tuned and calibrated for a cut-off size of 3 nm, a triple wavelength (467, 530, and 660 nm) particle/soot absorption photometer (PSAP; Radiance Research), a nephelometer (Radiance Research Model 903) using a wavelength of 545 nm, and an instrument system called the "aerosol package". In 2009, the aerosol package contained two

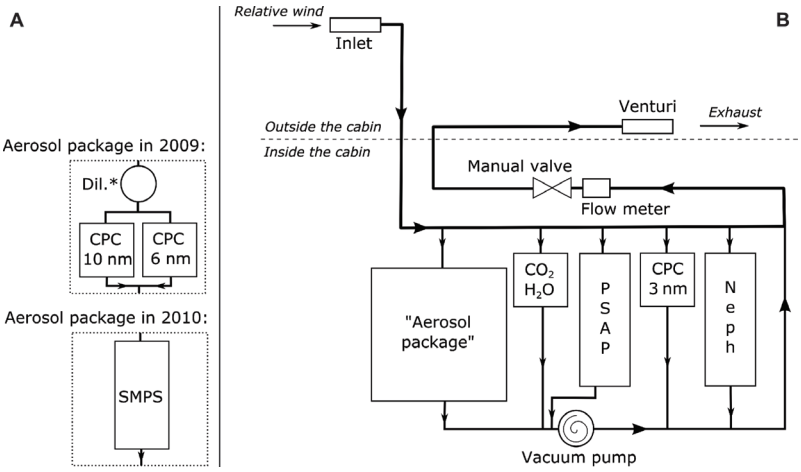


**Fig. 2**. (**A**) Schematic depiction of the flow system used on the measurement airplane, including an overview of the instruments located inside the aircraft. This is viewed from the top, and the airplane would be flying to the left, with the inlet mounted under the airplane's right wing. The dashed line represents the side wall of the cabin. (**B**) The two different options for the "aerosol package".

TSI 3772 CPCs, tuned and calibrated for cut-off sizes of 10 and 6 nm, respectively. The TSI 3772 CPCs are designed for maximum particle concentrations of $10^4$ $cm^{-3}$. For this reason, a dilution unit with a dilution factor of 1:10 could be optionally implemented in the sample line for these two instruments. (This dilution unit was used only until July 2009.) Henceforth, the collection of the two TSI 3772 CPCs and the TSI 3776 CPC that were used onboard the aircraft during 2009 will be referred to also as a "CPC battery". The time resolution of the all CPCs was one second, which meant a spatial resolution of 35 m.

For the measurements in 2010, the two TSI 3772 CPCs were replaced by a Scanning Mobility Particle Sizer (SMPS, Wang and Flagan 1990), consisting of a short Hauke-type DMA and a TSI 3010 CPC. The SMPS enabled us to measure the particle size distribution in the mobility diameter range from 10 to 350 nm with a time resolution of 2.1 minutes corresponding to a spatial resolution of 4.5 km. In addition to the size distributions obtained from the SMPS, we calculated the particle concentrations for an additional size bin by taking the difference between the total concentration as measured by the CPC (cut-off size of 3 nm) and the integrated concentration from the SMPS. The nominal particle size of that channel is 5.5 nm.

With the current instrumental setup, we were not able to measure aerosol size distribution for particles > 350 nm, however, from the shape of size distribution we can safely assess that they did not significantly contribute to total aerosol number densities. We inverted the SMPS data as described in Collins *et al*. (2002), and implemented calibration results as well as corrections for diffusion losses. The latter were estimated for the aerosol sample line used on the aircraft by assuming a turbulent flow in a straight tube (Hinds 1999). The penetration efficiencies were 69% and larger.

Note that due to the lack of ability to measure a complete aerosol number size distribution during observations carried out in 2009, no tube loss corrections were applied to any results on total number concentrations from 2009 (i.e. case studies 1 and 2). Concentrations for certain size bins, obtained by taking the difference of CPC counts, were however corrected for diffusional losses of particles of the respective mean size, again assuming turbulent flow in a straight tube. The penetration efficiencies for the used size bins range from 70% to 85%. The resultant numbers will be closer to the actual particle concentrations than the raw data, and are easier to compare with the corresponding results from the instrumentation used in 2010 (SMPS and CPC, case study 3).

The TSI 3772 model CPCs occasionally encountered problems at high altitudes (usually > 2 km), giving abnormally high (in particular higher than the 3 nm cut-off TSI 3776 CPC) and

erratic count rates. The corresponding data were excluded from the analysis, seen as occasional gaps in the presented data.

Both setups of the aerosol package and the LI-840 and the PSAP required an external vacuum that was provided by a vacuum pump (Thomas 107CDC20/12). The equipment further included a combined temperature/relative humidity (RH) sensor (Rotronic HygroClip-S) mounted on the airplane's right wing in an aluminum cover tube, underneath the sample air inlet (*see* Fig. 1). Unfortunately, due to the housing of the sensor, the actual time constant of the temperature/RH measurements was of the order of minutes, and the obtained data often not usable. A GPS receiver was used onboard to track the airplane's latitude, longitude, and altitude at a time resolution of one second. Data from all instruments were collected by a computer that was built into the rack and could be accessed remotely from the front seats by using a small laptop connected to the rack computer. This allowed for a continuous surveillance of the instruments during the flights. Starting from October 2010, a web camera was installed in the cockpit, close to the right-hand-side seat and pointing outside in the direction of the aerosol inlet. It took pictures every 30 s, providing information on prevailing cloud conditions. Electrical power (12 V DC) was provided by two rechargeable batteries, attached to the instrument rack.

During September 2009 and October 2010, the nephelometer and PSAP were not part of the setup.

### Ground-based instrumentation and models

The measurement flights presented in this study were supplemented by the data collected on the ground, in particular at the SMEAR-II station (Hari and Kulmala 2005). The SMEAR-II station is situated in Hyytiälä, Finland, in the boreal forest 50 km northeast of the city of Tampere, at an elevation of 179 m, and is home to a host of instrumentation. Extensive ambient aerosol measurements are performed continuously, as well as measurements of e.g. meteorological parameters and concentrations of trace gases. The data taken by size-resolving aerosol measurement instruments at the SMEAR-II station — in particular the Differential Mobility Particle Sizer (DMPS, Aalto *et al*. 2001) and various ion mobility spectrometers, such as the Balanced Scanning Mobility Analyzer (BSMA, Tammet 2006) and the Air Ion Spectrometer (AIS, Mirme *et al*. 2007) — allow for the detection and analysis of atmospheric new particle formation from gaseous precursors (Dal Maso *et al*. 2005) taking place at the location of sampling, i.e. inside the boreal forest. Data from the DMPS were used extensively in this study. It measures number size distributions in the range from 3 to 1000 nm at a time resolution of 10 min.

Backward trajectories were calculated using the Hybrid Single Particle Lagrangian Integrated Trajectory (HYSPLIT) model (publicly available at http://ready.arl.noaa.gov/HYSPLIT.php). Calculations were done for air masses ending over the SMEAR-II station at three altitudes during the time of the flight: close to the ground, upper boundary layer (1250 m), and lower free troposphere (2500 m).

Atmospheric soundings data were obtained twice a day (at 02:00 and 14:00) at Jokioinen, 75 km S of Tampere, 125 km from the SMEAR-II station. The data is publicly available at http://weather.uwyo.edu/.

## Results and discussion

Every flight utilizing the described setup was flown from and to the Tampere-Pirkkala Airport (ICAO-Code EFTP) in southern Finland. From 7 May 2009 to 21 Sep. 2009, a total of 18 measurement flights were performed. Thirteen measurement flights took place in October 2010. The total area covered reached from 23.5°E to 25.5°E and from to 61°N to 62.5°N (*see* the box in Fig. 3C). Most of the flights aimed at examining new particle formation in the boreal forest environment and were supplemented by data collected on the ground. The flights usually included climbs up to an altitude of 4 km and subsequent descents close to ground level, yielding both vertical and horizontal profiles of the measured

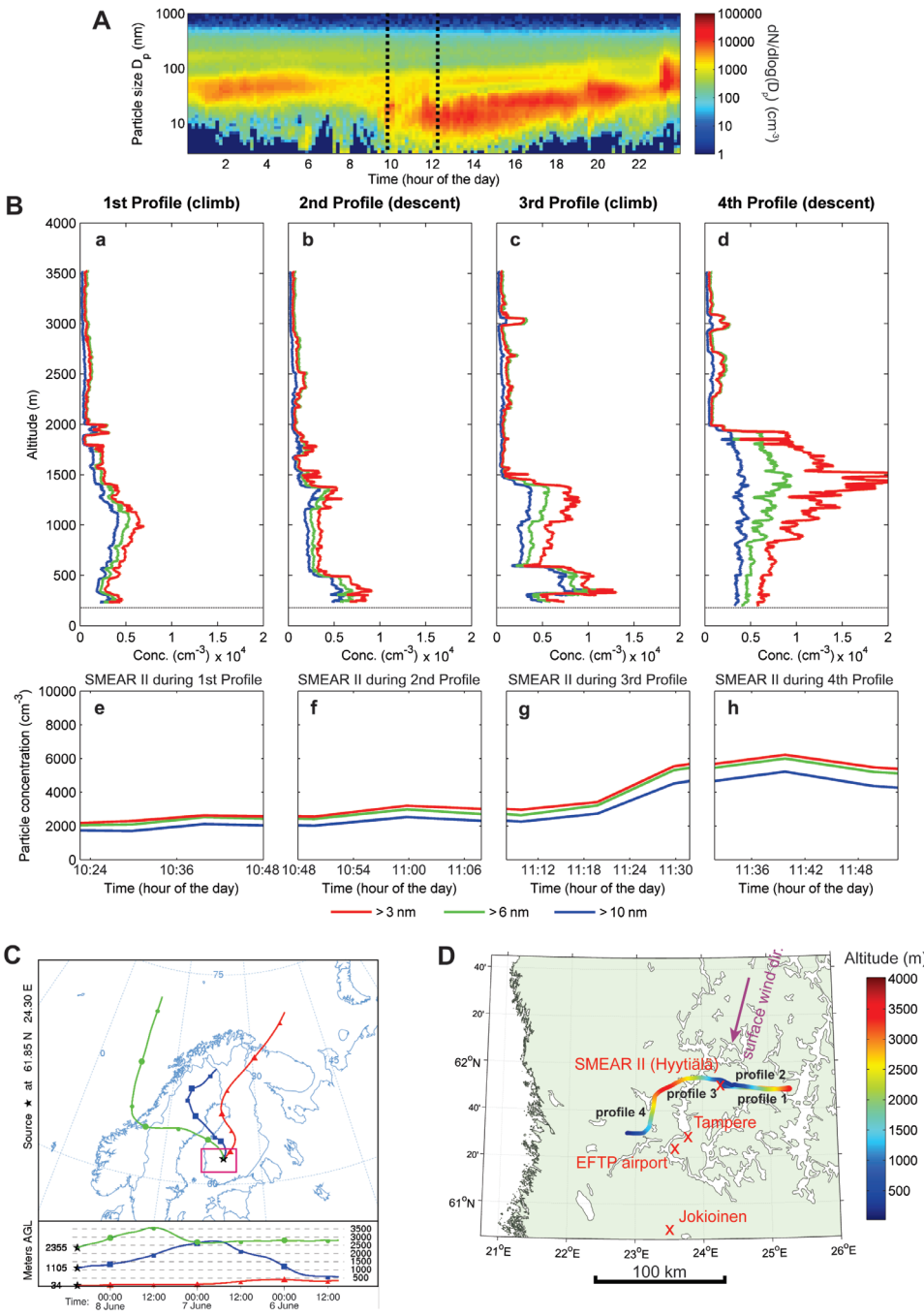


**Fig. 3**. (**A**) Particle size distribution as measured by the DMPS at the SMEAR-II station in Hyytiälä on 8 June 2009. The dotted lines mark take-off and landing of the measurement airplane. (**B**) **a**–**d**: particle concentrations for three size ranges measured by the CPCs onboard the aircraft (uncorrected) during the four vertical profiles of the flight; and **e**–**h**: corresponding particle concentrations obtained from integrating parts of the ground-based DMPS particle size distributions. Note that all particle concentrations are given normalized to 288.15 K of temperature and 1013.25 mbar of pressure. (**C**) 72-hour backward trajectories obtained from the HYSPLIT model for air masses ending at different altitudes over the SMEAR-II station at 11:00 local standard time (EET) [times shown in this plot are in UTC (EET – 2)]. The magenta box encompasses the area shown in panel **D**. (**D**) Map showing where the profiles were measured. Altitude is color-coded. The surface wind direction (at 34 m) at SMEAR II is shown in purple.

parameters. Most of these profiles started and/or ended at the SMEAR-II station allowing direct comparisons between airborne and ground measurements. Two sets of flights were conducted within a time span of about 24 hours (also during night time), in order to observe diurnal variations in the boundary layer and lower troposphere aerosol. Some flights aimed at taking measurements from plumes emitted by industrial facilities (e.g. power plants), and a series of flights investigated extensively the plumes of a controlled biomass burning experiment in Hyytiälä, Finland, on 26 June 2009. Details about the flights associated with this experiment and the results from them are found in Virkkula *et al*. (2011).

In general, particle measurements during the flights close to the forest canopy over the SMEAR-II station in Hyytiälä agreed well with the ground-based DMPS measurements. Another common observation made during many flights was high particle concentrations close to or downwind from the urban area around the city of Tampere. Data collected while flying low over these areas, which usually happened on all flights shortly after takeoff and before landing, were removed from this analysis, if a direct anthropogenic origin seemed likely.

All particle number concentrations presented are given normalized to a temperature of 288.15 K and a pressure of 1013.25 mbar, which results in only minor corrections due to low altitudes. Note that we chose 288.15 K as the standard temperature, which was closer to actual ambient temperatures at the surface, than the commonly used 273.15 K. The effects of this difference on the numbers presented are, however, minimal.

Altitudes are given in altitude above mean sea level, and all times are given as Eastern European Time (EET), i.e. UTC + 2, unless otherwise noted.

## Flights on days of a "new particle formation event": 3 case studies

Fourteen out of the total of 31 flights were conducted on days that can be clearly classified as class I or II "event days" by the DMPS results from SMEAR II. These are the days featuring a new particle formation events, i.e. a persistently growing new mode of particles < 25 nm (Dal Maso *et al*. 2005). A class II event differs from a class I event by strong fluctuations in the new, growing mode that make the growth rate determination impossible.

Here we focus on a total of seven flights on three case days (Table 1).

We chose the flight on 8 June 2009 for case study 1, because the flight took place just at the onset of the new particle formation event, as recorded at SMEAR II, and because all instruments were working without problems during that flight. The second case study is comprised of four flights on 21 and 22 Sep. 2009, which make up the first set of flights conducted within a 24-hour period with the first day being an event day. The first of these flights coincided with the onset of the NPF event, just as in case study 1.

Other event days in 2009, on which flights were performed, were not chosen because they were less successful in clearly observing new particle formation: The flight on 7 May 2009, for instance, was started too late, when the new particle formation (as measured by ground-based instruments at the SMEAR-II station) was already finished. The results from the flight on 18 May 2009 are in general similar to the presented case studies 1 and 2, but the NPF event recorded at SMEAR II was relatively weak and two of the CPCs had problems above 2 km. Combinations of bad timing, weak or strongly fluctuating nucleation events, and instrumental problems, also disfavored the three flights on 25 and 26 May 2009.

Case study 3 presents results from two flights in 2010, employing the SMPS. The meteorological conditions and the NPF events on 11, 12 and 13 Oct. 2010 were relatively similar. The last one of these events was chosen for detailed representation as case study 3 due to the most complete data set collected during that day.

### Case study 1 (8 June 2009): Regional NPF event in late spring

On 8 June 2009, a class I (Dal Maso *et al*. 2005) particle formation event was recorded at the SMEAR-II station, as can be seen by the results from the ground-based DMPS of that day

**Table 1**. Summary of the 7 measurement flights presented in the three case studies, as well as information regarding the flights and other measurements during the day. Times are given in EET (UTC + 2). Events were classified as explained in the text (*see* section 'Flights on days of a "new particle formation event": 3 case studies'). Wind data are averages over the times of the respective flight. An asterisk (*) denotes information that was obtained from Tampere-Pirkkala airport (when data from SMEAR II was not available). Air mass origins are derived from the HYSPLIT backward trajectory model results ending at the SMEAR-II station during the times of the flights (as presented in the text and in Figs. 3C, 6C, and 7C). Information on cloud cover (right-most column) is presented in octas of coverage for each particular layer of cloud (e.g. 4/8 if the layer covered 50% of the sky).

| Case study | Time of flight | Description of Flight | Data from SMEAR-II station (Hyytiälä) | | | Cloud information (Sources: 2009: EFTP airport; 2010: airborne camera) |
|---|---|---|---|---|---|---|
| | | | NPF event | Wind (34 m) direction and speed | Air mass origin (HYSPLIT, 34 m) | |
| 1 | 8 June 2009, 09:55–12:10 | 4 vertical profiles (altitude < 4 km) E and W from and to SMEAR II, passing SMEAR II twice at low level | class I, start 10:30 | 015°, 2.8 m $s^{-1}$ | Arctic Sea; over N Finland for > 60 hours | At first, sky clear; clouds, starting from 11:30, 1/8–5/8, cloud base at 2000 m |
| 2 | 21 Sep. 2009, 12:45–15:20 | 4 profiles (altitude < 4 km) NW and S of SMEAR II, passing SMEAR II at low level | class I, start 13:45 | 274°, 3.7 m $s^{-1}$ | North Atlantic; over central Sweden/Norway for > 24 hours | Sky clear |
| 2 | 21 Sep. 2009, 17:45–19:40 | 4 profiles (altitude < 4 km) WNW and S of SMEAR II, passing SMEAR II at low level | | 261°, 2.9 m $s^{-1}$ | | 2 layers of cloud: 1/8–5/8, cloud base at 2100 m, 3/8–7/8, cloud base at 4300 m |
| 2 | 21 Sep. 2009, 22:20–00:15 | 4 profiles (altitude < 4 km) NW and S of SMEAR II, passing SMEAR II at low level | | 239°, 3.5 m $s^{-1}$ | | At first, 3 layers of cloud: 1/8–3/8, cloud base at 450 m, 3/8–5/8, cloud base at 750 m, 3/8–7/8, cloud base at 1500 m, dissolving between 23:00 and 00:00, then sky clear |
| 2 | 22 Sep. 2009, 11:10–12:25 | 2 profiles (altitude < 4 km) WNW of SMEAR II | undefined | 204°, 4.6 m $s^{-1}$* | | 3 layers of cloud: 1/8, cloud base 800 m, 3/8, cloud base 1000 m, dissolving around 12:00, 5/8–8/8, cloud base 1500 m |
| 3 | 13 Oct. 2010, 07:42–10:15 | 2 profiles (altitude < 4 km) to E and SE of Tampere and SMEAR II | class II, start 10:00 | 303°, 3.8 m $s^{-1}$ | Arctic Sea; over N Scandivia for ca. 24 hours | Sky clear |
| 3 | 13 Oct. 2010, 12:29–14:59 | 2 profiles (altitude < 4 km) W and NW of SMEAR II, passing SMEAR II at low level | | 313°, 5.1 m $s^{-1}$ | | At airport: few clouds (1/8), cloud base 900–1100; at SMEAR II: scattered cloud layer, base at 800–1000 m |

(Fig. 3A; the times of beginning and end of the flight are marked by dashed lines). The possibility of observing steady nucleation and growth on the ground over many hours requires uniformity of the NPF event over a certain area, therefore a regional character of the event was expected. Backward trajectory calculations place the origin of the measured air masses over the Arctic Ocean (Fig. 3C). The air that was most likely very clean then passed over land, mostly over boreal forest, before reaching southern Finland 40–60 hours later (depending on altitude). This kind of air mass history is frequently associated with the detection of atmospheric new particle formation at the SMEAR-II station (Nilsson *et al*. 2001a, Sogacheva *et al*. 2005).

The airborne CPC battery results from four vertical profiles for the concentrations of particles > 3 nm, > 6 nm, and > 10 nm are shown in Fig. 3B. For comparison, we calculated ground-level concentrations by integrating the particle size distributions measured by the ground-based DMPS at corresponding times (Fig. 3Be–h), and the thereby derived aerosol number densities correspond to submicron aerosol with minimum size limit 3, 6, and 10 nm respectively. The vertical profiles were taken north of Tampere and close to the SMEAR-II station (Fig. 3C and D). Airborne measurements of water vapor and $CO_2$ concentrations are presented as a function of altitude (*see* Fig. 4A–D). The most prominent features of these profiles were a marked decrease/increase in [$H_2O$] when climbing/descending through a certain altitude, and often a concurrent increase/decrease of [$CO_2$]. This change between an air mass in closer exchange with the surface (evaporation of water, uptake of $CO_2$) to a drier air mass above served as our definition of the height of the boundary layer, namely (for profiles 1–4) at about 1800, 1600, 1500 and 2000 m. A sounding made in Jokioinen about 3 hours after the flight, at 14:00, showed a constant potential temperature profile up to 1900 m, supporting the choices made based upon the $H_2O$ and $CO_2$ profiles (Fig. 4E).

The aerosol number concentrations vertical profiles usually exhibited a marked decrease when climbing from the boundary layer into the free troposphere. The results clearly showed the presence of particles in the size ranges 3–6 nm and 6–10 nm throughout the boundary layer. There was a general increase in the particle concentrations over time (Fig. 3Ba–d and e–h from left to right), in agreement with the ground-based DMPS measurements. One difference was in the increase in concentrations of small particles (3–6 nm and 6–10 nm) at the start of the NPF event (which occurred during the time of the flight), which was much less prominent on the ground. The measured concentrations in the boundary layer varied noticeably also in location and altitude (Fig. 3B and D). The difference between measured concentrations of 3–6 nm particles and concentrations observed on the ground reached values of up to about 8100 per $cm^3$, corresponding to a more than 30-fold increase, with a maximum at an altitude of around 1500 m (Fig. 5A). In the 6–10 nm range, the difference in particle concentration was up to about 3900 $cm^{-3}$, corresponding to a more than four-fold increase. Also, the total aerosol concentrations were higher in the boundary layer than on the ground (even without taking tube losses into account which would magnify the observed pattern).

Particle number concentrations above the boundary layer were much smaller, and particles < 6 nm were absent, indicative of the absence of recent new-particle formation.

The reasons for the inhomogeneities in the particle concentrations in the boundary layer could not be ascertained with the current instrumental setup. Moreover, on a horizontal scale, the vertical profiles were flown 50 km to the east of the SMEAR-II station (1st profile), back (2nd profile), and then 90 km to the west-southwest (3rd and 4th profile). The flight paths were oriented perpendicular to prevailing light northerly winds [2.8 m $s^{-1}$ close to the surface (Table 1)]. The landscape overflown (and that to the north of the flight paths) is predominated by boreal forest, but features intermittent lakes, swamps, and agricultural land. So the simplest conceivable cause of these variations is geographical variations in these areas. Concentrations of trace gases usually connected with new particle formation (such as sulfuric acid and volatile organic compounds) were not measured onboard; however it seems plausible that they varied between the sampled air masses in the boundary layer. Indeed, variations in the water vapor and $CO_2$ concentration

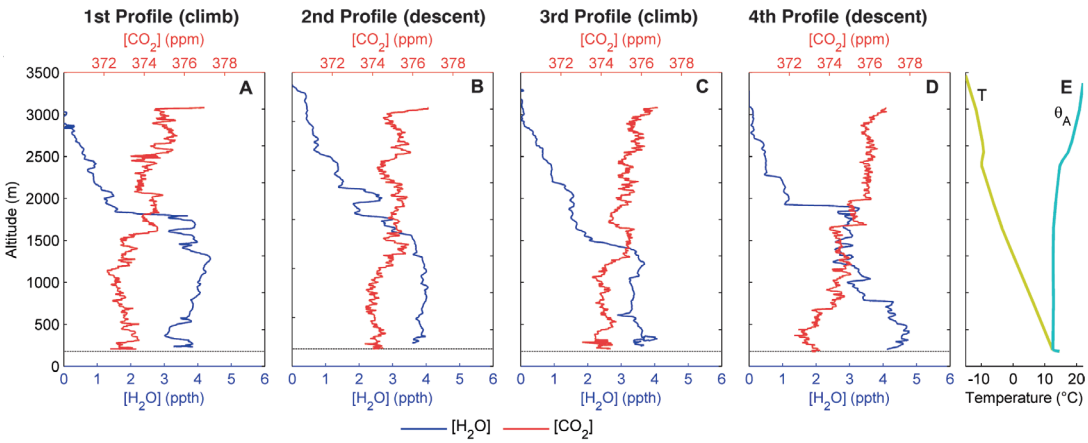


**Fig. 4**. (**A–D**) Water vapor and $CO_2$ concentrations measured by the LI-COR, along the four vertical profiles of the flight of case study 1 (compare Fig. 3) on 8 June 2009. (**E**) Temperature (T) and potential temperature ($\theta_A$) were obtained by sounding at Jokioinen on 8 June 2009 at 14:00.

profiles often suggested a non-uniform mixing of the boundary layer (Fig. 4). Boundary layer dynamics (turbulence, entrainment) therefore appeared to play a role. They were not directly investigated by our instrumentation, but were previously suggested to play an important role in boundary-layer nucleation (Nilsson *et al*. 2001b, Crippa *et al*. 2012). Entrainment fluxes at the top of the boundary layer, for instance, may cause temperature fluctuations creating a more suitable environment for nucleation and early growth by condensable vapors. Evidence for entrainment-induced new particle formation was also reported by others (*see* e.g. Wehner *et al*. 2010, Pryor *et al*. 2011). Unless regional variations were dominating in our measurements, this hypothesis is in agreement with our observation of concentrations of 3–6 nm particles being mostly higher in the upper half of the boundary layer. A prime example is the 4th profile, with very high counts of 3–6 nm and 6–10 nm particles between 800 m and 2000 m (the top of the boundary layer), and lower counts below. Note that the described pattern was not observed for presumably older (grown) particles > 10 nm. A transition at 800 m was also seen in the $H_2O$ and $CO_2$ profiles, with lower [$H_2O$] and higher [$CO_2$] above, suggesting that the air mass above 800 m experienced a less recent exchange with the surface, and a more recent mixing with the free troposphere on top.

## Case study 2 (21–22 Sep. 2009): Diurnal pattern during a regional NPF event in autumn

A set of four flights was conducted within 24 hours during 21 and 22 Sep. 2009. On each of the first three flights, four vertical profiles were flown with near-identical flight paths (Fig. 6D). For the last flight (morning of 22 Sep.), only two profiles were flown, along path 1 (climb) and back (descent). The airborne CPC battery measurements were summarized by averaging over all profiles for each flight, and averaged over 100 m steps in altitude (Fig. 6Bb–e). The data from low altitudes close to the airport or the city of Tampere were excluded, as well as some data from TSI 3772 CPCs during malfunctions of the respective instrument.

The first of the four flights was conducted during the onset of a new particle formation event. Using the DMPS data from the SMEAR-II station in Hyytiälä (Fig. 6A), it was classified as a class I event, and appeared very similar to the event in case study 1. Again, a regional character of the NPF event was expected. The air mass history was also similar to case study 1. According to the backward trajectory model (Fig. 6C), the measured air masses originated from the North Atlantic Ocean, approximately at 60°N. The air masses passed over land for at least 24 hours before reaching central-southern

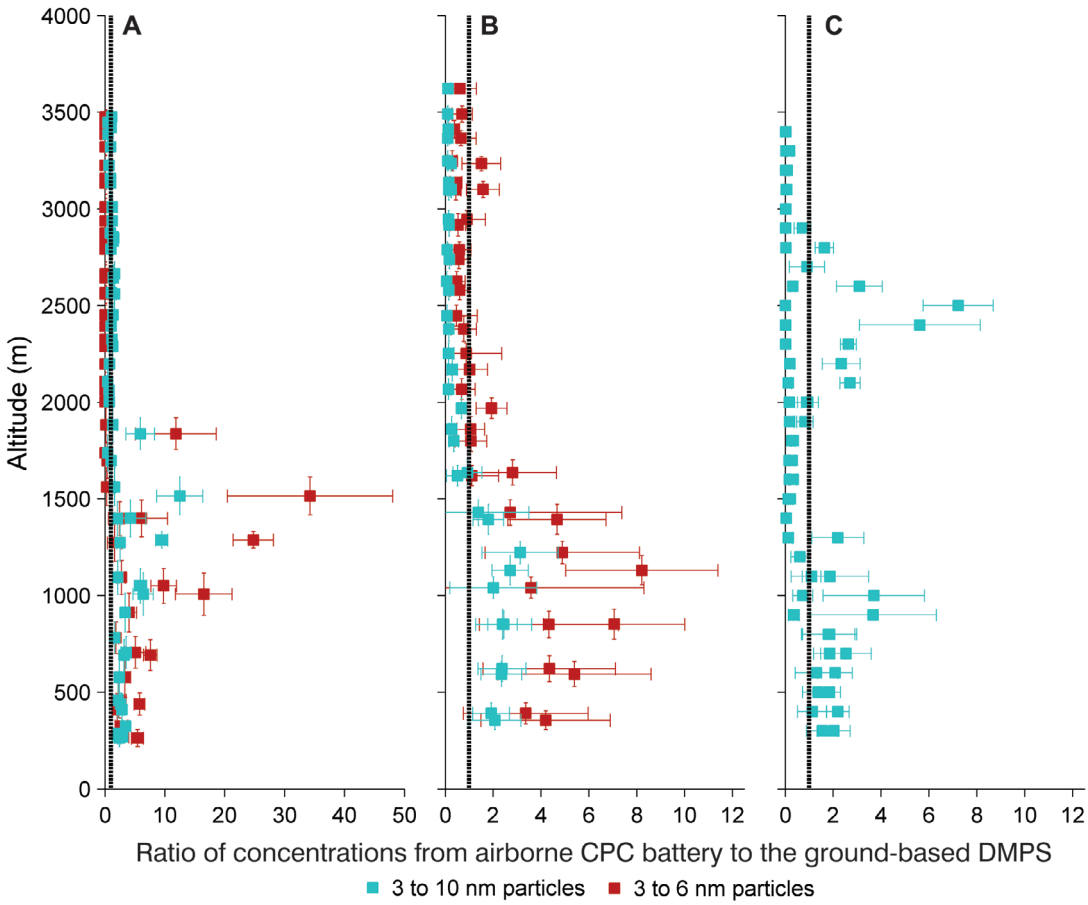


**Fig. 5**. Concentrations of 3–6 nm and 3–10 nm particles (corrected for diffusion losses in the sampling line), measured at different altitudes during (**A**) case study 1, (**B**) the first flight of case study 2, and (**C**) the second flight of case study 3, normalized by the corresponding measurements by the DMPS at SMEAR II at same times (but notably not same locations). Each presented data point was calculated using interpolated ground-based DMPS measurements (10 min time resolution), and either (case studies 1 and 2) 100s of airborne CPC measurements (1 s time resolution) or (case study 3) fixed altitude bins of a width of 100 m. Error bars are the sample standard deviations. Note that all particle concentrations have been normalized to 288.15 K of temperature and 1013.25 mbar of pressure.

Finland. Similar to case study 1, the flight paths were perpendicular to the prevailing wind direction (Fig. 6D).

In the first flight, the number concentrations of particles in the size ranges 3 to 6 nm and 6 to 10 nm were high (as compared with those in the three later flights), typical of on-going new particle formation. As compared with those in case study 1, the concentrations of particles in this size range from the airborne measurements were closer to those measured on the ground during this flight, but still higher (Fig. 5B). Again there were pronounced drops in particle number concentrations above 1000 to 1500 m. Unfortunately, the airborne [$CO_2$] and [$H_2O$] measurements were not working during this flight (or any of the 4 flights of this case study), so the only evidence for an increased stability above about 1000 m came from the sounding in Jokioinen during the flight (Fig. 6Ba). Based on the airborne observations and soundings, we therefore assume that the decrease in particle concentrations marked the top of the boundary layer.

There was also a remarkable variation of the measured particle concentrations in the boundary layer with location and altitude. Unlike in

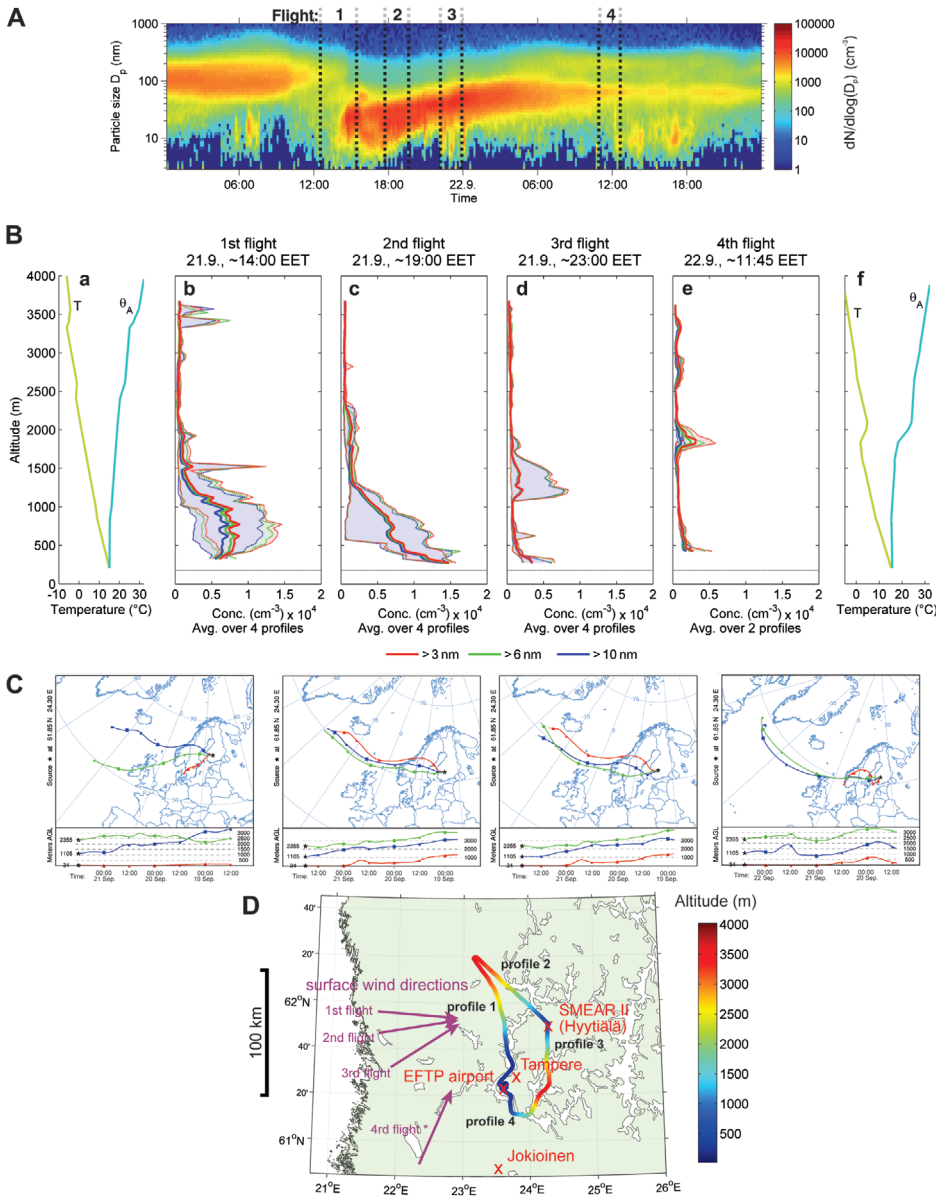


**Fig. 6**. (**A**) Particle size distribution measured by the DMPS at the SMEAR-II station in Hyytiälä during 21–22 Sep. 2009. The dotted lines mark take-off and landing times of the measurement airplane. (**B**) **b**–**e**: vertical particle concentration profiles (uncorrected) measured by the CPCs onboard the aircraft for each of the four flights in chronological order (from left to right), averaged over altitude in 100-m steps; thick lines represent averages over all four vertical profiles of each flight (except only two profiles for the fourth flight); dashed lines show the maximum and minimum values measured during each flight; areas between thin lines have been colored to guide the eye. Note that all particle concentrations are given normalized to 288.15 K of temperature and 1013.25 mbar of pressure. **a** and **f**: the results of sounding in Jokioinen (**a**) on 21 Sep. at 14:00 during the first flight, and (**f**) on 22 Sep. at 14:00 2 hours after the fourth flight. (**C**) 72-hour backward trajectory calculations for each of the four flights, ending over the SMEAR-II station on 21 Sep. on 14:00 EET, 20:00 EET, 23:00 EET, and on 22 Sep. at 12:00 EET. However, times shown on the four plots are in UTC (EET – 2). (**D**) Map showing where the profiles were flown during the first flight. Altitude is color-coded. The flight paths for the second and third flights were very similar. During the fourth flight, only two profiles were flown, approximately along the path of the first profile of the first three flights. Surface wind directions (at 34 m at SMEAR II during the first three flights and at Tampere-Pirkkala during the fourth flight) are displayed in purple.

case study 1, most of this variation was in particles > 10 nm. For instance, at an altitude of 800 m and practically at the same time (7.5 min apart), the total particle concentrations were > 10 000 $cm^{-3}$ about 20 km NW of Hyytiälä, and only around 5000 $cm^{-3}$ about 20 km south of Hyytiälä. Variations in air mass origin are the most likely explanation. Smaller particles (3–10 nm, possibly recently created by atmospheric nucleation) showed less variation. Their numbers were mostly constant around 1000 $cm^{-3}$ during the profiles 2 and 3 (close to SMEAR II), and varied between 2100 and 3300 $cm^{-3}$ during the profiles 1 and 4, i.e. about 30 km farther upwind. Assuming a wind speed of 3.7 m $s^{-1}$ (i.e. the prevailing surface wind), this distance corresponded to a travel time of 2 h 15 min. Allowing for an actual wind speed of up to double the surface wind speed (due to surface roughness, surface winds are often slower than winds aloft), the estimated travel time is between one and two hours.

The growth rate determined from the ground-based DMPS measurements was 6.7 nm $h^{-1}$ for the size range 3–20 nm [determined as in Yli-Juuti *et al*. (2011)], so one to two hours was then enough for almost all the 3–10 nm particles to grow into sizes > 10 nm. One possible explanation for most of the observed variation in particles concentrations in this size range would therefore be a stronger NPF (i.e. higher formation rate) about 30 km to the east of the SMEAR-II station. Another explanation is that the variability in condensing vapors concentration and different partitioning of semi-volatile compounds are causing this pattern, although we cannot address this possibility with the instrumental setup used in this study.

The subsequent two flights did not find any more boundary layer NPF. During the night flight (flight 3), remarkably high particle concentrations (peaks at 8400 $cm^{-3}$, particle sizes mostly > 10 nm) between 1100 and 1900 m were observed around 50 km north of Tampere (profile 1). For comparison, clean troposphere background concentrations were below 500 $cm^{-3}$ (measured about 20 km to the east). In this case, a temperature inversion was observed above 1900 m by the onboard instrumentation (despite the large time constant of the onboard temperature sensor), suggesting that the increased particle counts were due to an aerosol layer or plume trapped by the inversion. The absence of these high concentrations in profiles 2–4 limited the horizontal extent of this layer somewhat.

During the fourth flight, we observed an unexpected layer of particles about 50 km north of Tampere in the free troposphere, between altitudes 1700 m and 2100 m, including nucleation mode (i.e. < 10 nm and < 6 nm) particles (Fig. 6Be). A broken (7/8) cloud layer was observed right below the location of this layer (cloud base of 1400–1680 m measured at Tampere-Pirkkala airport), while the Jokioinen sounding two hours after the flight showed a temperature inversion from 1800 to 2100 m. The small size of the observed particles suggested nucleation as their source, with the inversion possibly increasing their concentration locally. There have been previous observations of local new particle formation exclusive to certain regions in the atmosphere associated with turbulence and/or cloud: Wehner *et al*. (2010) presented observations of a particle mode < 10 nm in patches in the residual layer during the morning time, suggesting that these particles were indicative of new particle formation due to turbulent conditions locally ameliorating the conditions in favor of new particle formation. It has also been discussed how new particle formation takes place in the outflow of convective clouds (e.g. Clement *et al*. 2002), and Weber *et al*. (2001) observed new particle formation above a frontal cloud, coincident with locally increased sulfuric acid concentrations.

## Case study 3 (13 Oct. 2010): Regional NPF event in autumn 2010

On 13 Oct. 2010, a new particle formation (NPF) event was observed at the SMEAR-II station in Hyytiälä, starting around 10:00, with the growth of newly formed particles continuing until 20:00. Two measurement flights were flown during that day, partially concurrent with the NPF event (Fig. 7A; start and end times for profile pairs 1 and 2, and 3 and 4 are marked by vertical lines). The first flight took place between 08:00 and 11:00, and followed a route to the southeast of Tampere and did not pass close to Hyytiälä. The

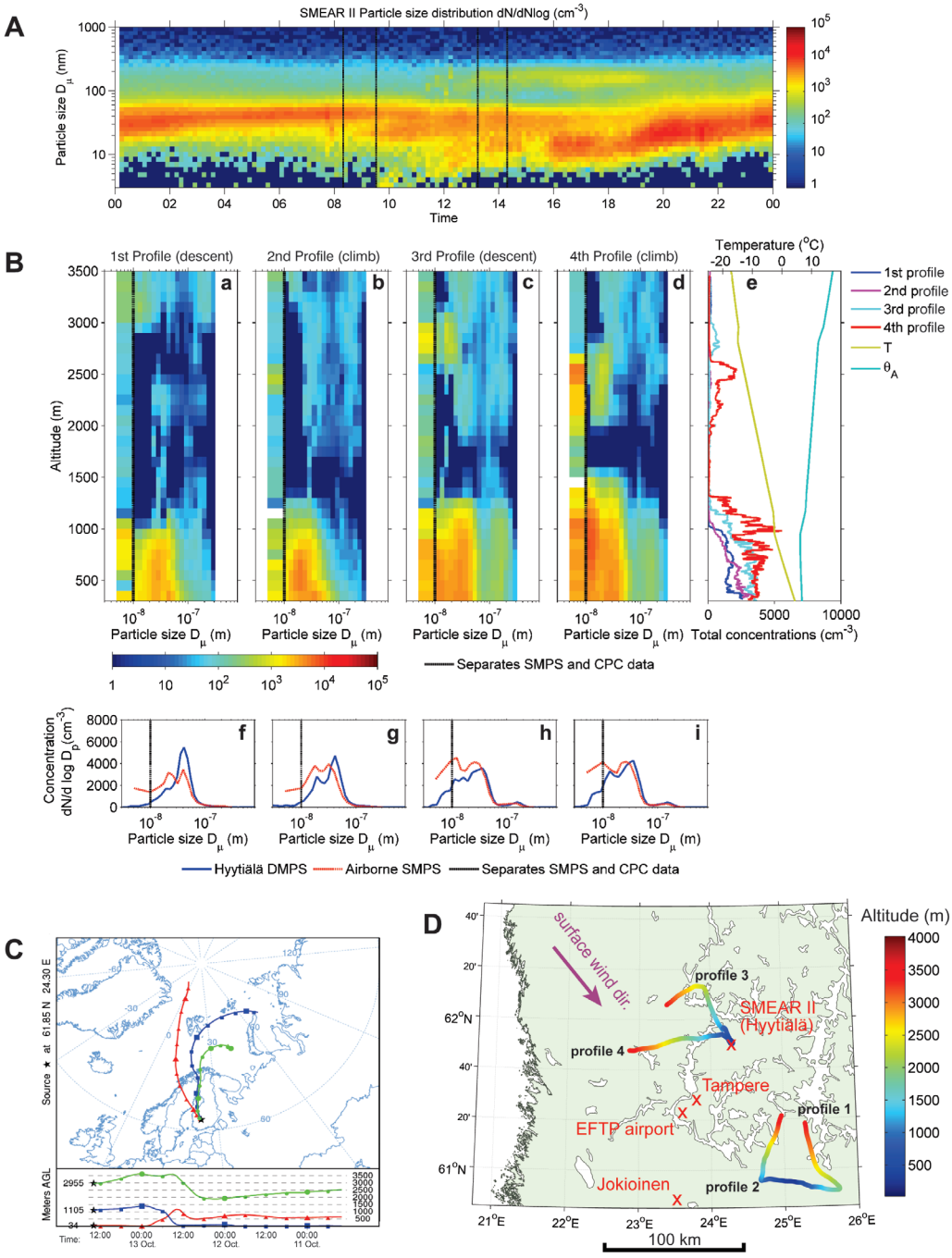


**Fig. 7**. (**A**) Particle size distribution measured by the DMPS at the SMEAR-II station in Hyytiälä on 13 Oct. 2010. The airborne measurements are performed during the time between the vertical lines. (**B**) **a**–**d**: particle size distribution measured by the stand-alone CPC and the SMPS onboard the aircraft during the four vertical profiles (corrected); (**e**) the total concentrations during the profiles, measured by the stand-alone CPC (> 3 nm, uncorrected), and the results of the soundings in Jokioinen at 14:00 during the second flight; **f**–**i**: particle size distributions of the lowest measured altitude compared with the average particle size distribution at Hyytiälä during the time of the corresponding profile measured by the DMPS. (**C**) 72-hour backward trajectories obtained from the HYSPLIT model for air masses ending at different altitudes over the SMEAR-II station at 14:00 local time. Times shown in this plot are in UTC (EET – 2). (**D**) Map showing where the profiles were flown, with the altitudes color-coded.

second flight on that day took place between 13:00 and 15:00, passing the SMEAR-II station at low altitude (Fig. 7A and D). Four vertical profiles were flown during each flight. In both cases, because the first and the fourth profiles were flown close to Tampere and therefore affected by anthropogenic sources of aerosol, the analysis focused on the first descent and second climb of each flight. In this study, we refer to them as profiles 1–4. Profiles 1 and 2 were flown just before the time of the first observations of fresh 3-nm particles at SMEAR II. Between the profiles 3 and 4, the nucleation mode was observed to grow in size (Fig. 7A). This timing allowed us to compare the situation before the NPF event with the later situation of an on-going growth of nucleation mode particles. The event at the SMEAR-II station was classified as a class II event, i.e. a new and growing mode of sub-25-nm particles could be observed, but the growth rate and the formation rate parameters could not be determined with a good confidence level (Dal Maso *et al*. 2005).

The wind direction during the flights was from the north and the air masses arriving at the SMEAR-II station originated from the Arctic Ocean (Fig. 7C), similar to the situation on 8 June 2009 (Fig. 3C). The air masses had spent around 24 hours over land before reaching central-southern Finland. Particle size distributions from 3 to 350 nm and total particle concentrations (> 3 nm) were measured using the SMPS combined with a stand-alone CPC for each of the four profiles (Fig. 7Ba–e). We calculated the average size distributions over altitude bins of 100 m between the altitudes 300–3500 m. The number concentrations in the lowest measured size bin (3–10 nm) were in general higher during the latter profile pair than during the first two profiles, agreeing with the timing of the first profiles before the observed new particle formation. The concentrations were also seen to increase from profile 3 to profile 4. For airborne and simultaneously measured on-ground concentrations of 3–10 nm particles, the airborne concentrations were again higher than the ones measured on ground (Fig. 5C), similar to case study 2. The atmospheric sounding, performed at Jokioinen at 14:00, simultaneously with the second flight, showed a constant potential temperature profile up to 1000 m, giving an indication of the boundary layer height. (Unfortunately, neither [$CO_2$] nor [$H_2O$] information is available from these flights to confirm the estimate of the boundary layer height.) A drop in observed concentrations near the SMEAR-II station occurred at a slightly higher altitude of around 1200 m. This difference can be explained by regional variation. During the first flight of the day, aerosol concentrations dropped at 1000 m, i.e. 200 m lower than during the second flight, corresponding to the assumption that the height of the boundary layer rose during the day. Variations of concentrations within the boundary layer at different locations were also apparent, such as an increase of concentrations from profile 3 to profile 4, noticeably not homogeneously with altitude.

The airborne particle size distribution measured at low altitude (300 m) above the tree canopy were compared with the distribution measured at the SMEAR-II station inside the canopy (Fig. 7Bf–i). Note that during the 1st and 2nd profiles, the distance to the SMEAR-II station was around 110 km, whereas the 3rd and 4th profiles passed the SMEAR-II measurement tower at the distances of 1.3 km and 0.8 km, respectively. The airborne total concentrations were higher than those simultaneously measured at SMEAR II, namely 2900 *vs*. 2000 $cm^{-3}$ (profiles 1 and 2), and 4200 *vs*. 3000 $cm^{-3}$ (profiles 3 and 4). The accumulation mode (particle diameters of 80–350 nm) compared very well, whereas concentrations of sub-25-nm particles were always higher in airborne than in ground-based measurements. This agreed with the observations on the 3–6 nm and 3–10 nm size channels during case studies 1 and 2. The shape of the aerosol size distribution measured at 300 m compared well to the ground observations during all four profiles suggesting a certain uniformity of aerosol in the air mass over horizontal distances well over 100 km.

There was a tendency for the modes of the particle size distributions from the airborne measurements to be shifted towards smaller sizes when compared with those from the ground-based measurements. This effect was most notable in profiles 2, 3, and 4, where the Aitken mode (20–80 nm) diameter from the airborne measurements is about 10 nm smaller than from

the ground-based measurements. The reason behind this effect remains unknown, and because this shift in size showed a rather stable pattern independent of altitude, we believe that it was caused by instrumental uncertainty. This shift also affects the aerosol concentrations of the lowest bin derived from the difference between total CPC counts and integral aerosol concentrations from the size distributions: The net effect would reduce the $dN/d\log D_p$ values of the lowest bin by up to around 30%, now covering the size range 3–20 nm, instead of 3–10 nm.

The vertical profiles of the particle size distributions themselves exhibited notable variations within the boundary layer (Fig. 7Ba–e). In profiles 1 and 2, the Aitken mode diameter seemingly steps towards a smaller size above about 500 m. In profile 4, the highest concentrations of sub-20-nm particles were observed between 700 and 1100 m, while the concentrations of Aitken and accumulation mode particles were decreasing with increasing altitude. The increase of nucleation mode particles indicated new particle formation proceeding at an increased rate at these altitudes. The reduced number of Aitken and accumulation mode particles indeed constituted a favouring factor for new particle formation due to reduced condensation and coagulation sinks, and may have been due to cloud processes. A layer of scattered stratocumulus (non-precipitating) was present in the area near the SMEAR-II station with the cloud base between 800 and 1000 m and the thickness of the layer in the order of 100–200 m.

At higher altitudes (up to the flights' ceiling of 3500 m), concentrations started to rise again, but staying mostly below 300 $cm^{-3}$. The most significant exceptions to that were observed between 2700 and 3000 m in profile 3 and between 2000 and 2600 m in profile 4. An atmospheric sounding performed at Jokioinen revealed an inversion layer situated at 2800–3000 m, suggesting that the observed layers of increased particle numbers concentrations in the free troposphere was due to aerosol trapped underneath the inversion. Also the onboard temperature sensor suggested an inversion layer at these altitudes. The observed particles were mainly sub-30 nm, so they could be freshly formed particles.

## Conclusions

Vertical profiles of aerosol number concentrations, including in 6–10 nm and 3–6 nm size ranges, and during some flights particle size distributions from 3 to 350 nm were successfully measured during airborne observations in 2009 and 2010, within about 200 km of the SMEAR-II measurement station in Hyytiälä, southern Finland.

Our measurements suggest that new particle formation events do not happen only close to the ground, but throughout the planetary boundary layer. It was also evident that this kind of new particle formation is a regional rather than a local phenomenon, as has been reported earlier e.g. by Hussein *et al*. (2009). Particle concentrations above the boundary layer were usually about an order of magnitude smaller indicating that the large-scale boundary layer new particle formation did not extend into the free troposphere.

The vertical distribution of aerosol particles within the boundary layer showed variations with altitude and horizontal location, which is also reflected in the variability of the aerosol particle number size distributions detected at the ground level. Geographical variations may have played a role in the observed variability, but no corresponding links could be established. Although the flight paths during our measurements cannot prove the actual absence of links to geographical features, at least some of the observed variability in aerosol particle size distributions was connected to boundary layer dynamics (case 1). In addition, changes in the intensity of new particle formation events with time and in space contribute to the observed variability, as seen during case 2 in this study. Previous airborne measurements over boreal forest (O'Dowd *et al*. 2009) found the largest concentrations of nucleation mode particles at very low altitudes, < 100 m above ground. Our results however did not reproduce these previous observations. Instead, an increase in concentration of newly formed aerosol particles was often observed towards the upper parts of the planetary boundary layer. Particle number concentrations measured in-flight during new particle formation (in particular for sizes < 10 nm) were sometimes considerably higher as com-

pared with numbers obtained from ground-based measurements. This is true for all three presented case studies. Our results might be attributable to entrainment fluxes, previously hypothesized to be beneficial to new particle formation. Measurements of particles size distributions revealed variations in the distribution of larger particle sizes as well, which were tentatively linked to cloud processing/removal.

On at least one occasion we found indications of a case of new particle formation occurring in the free troposphere and above clouds, within a confined altitude range.

This study delivered new information about the spatial extend of new particle formation in the boreal forest environment, but understanding of the processes behind the observed pattern needs further study.

*Acknowledgements*: We thank Erkki Järvinen and his team at Air Spark Oy for operating the measurement aircraft and their support, Tuomo Nieminen for providing calculated growth rates and condensation sinks, Petri Keronen for his help with interpreting the LI-COR data, Pirkko Karlsson and the Finnish Meteorological Institute for providing meteorological data from Tampere-Pirkkala airport for all flight days, the National Oceanic and Atmospheric Administration's Air Resources Laboratory for the Hybrid Single Particle Lagrangian Integrated Trajectory (HYSPLIT) trajectory model (available at http://ready.arl.noaa.gov/HYSPLIT.php), and the University of Wyoming's Department of Atmospheric Sciences for data from atmospheric soundings (available at http://weather.uwyo.edu/upperair/sounding.html). This work was supported by the European Commission 6th Framework program (contract no. 036833-2: EUCAARI), the European Commission 7th Framework program (grant agreement number 215072: Marie Curie Initial Training Network, CLOUD-ITN), and the European Research Council (ERC-ATMNUCLE). The financial support by the Academy of Finland Centre of Excellence program (project no. 1118615) is gratefully acknowledged.

## References

Aalto P.P., Hämeri K., Becker E., Weber R., Salm J., Mäkelä J.M., Hoell C., O'Dowd C.D., Karlsson H., Hansson H.-C., Väkevä M., Koponen I.K., Buzorius G. & Kulmala M. 2001. Physical characterization of aerosol particles during nucleation events. *Tellus* 53B: 344–358.

Arneth A., Unger N., Kulmala M. & Andreae M.O. 2009. Clean the air, heat the planet? *Science* 326: 672–673.

Baumgardner D., Brenguier J.L., Bucholtz A., Coe H., DeMott P., Garrett T.J., Gayet J.F., Hermann M., Heymsfield A., Korolev A., Krämer M., Petzold A., Strapp W., Pilewskie P., Taylor J., Twohy C., Wendisch M., Bachalo W. & Chuang P. 2011. Airborne instruments to measure atmospheric aerosol particles, clouds and radiation: A cook's tour of mature and emerging technology. *Atmos. Res.* 102: 10–29.

Boy M., Petäjä T., Dal Maso M., Rannik Ü., Rinne J., Aalto P., Laaksonen A., Vaattovaara P., Joutsensaari J., Hoffmann T., Warnke J., Apostolaki M., Stephanou E.G., Tsapakis M., Kouvarakis A., Pio C., Carvalho A., Römpp A., Moortgat G., Spirig C., Guenther A., Greenberg J., Ciccioli P. & Kulmala M. 2004. Overview of the field measurement campaign in Hyytiälä, August 2001 in the framework of the EU project OSOA. *Atmos. Chem. Phys.* 4: 657–678.

Brook R.D., Rajagopalan S., Pope A.III, Brook J.R., Bhatnagar A., Diez-Roux A.V., Holguin F., Hong Y., Luepker R.V., Mittleman M.A., Peters A., Siscovick D., Smith S.C.Jr., Whitsel L. & Kaufman J.D. 2010. Particulate matter air pollution and cardiovascular disease, an update to the scientific statement from the American Heart Association. *Circulation* 121: 2331–2378.

Buzorius G., McNaughton C.S., Clarke A.D., Covert D.S., Blomquist B., Nielsen K. & Brechtel F.J. 2004. Secondary aerosol formation in continental outflow conditions during ACE-Asia. *J. Geophys. Res.* 109: D24203.

Clarke A.D. 1992. Atmospheric nuclei in the remote free-troposphere. *J. Atmos. Chem.* 14: 479–488.

Clarke A.D. & Kapustin V. 2010. Hemispheric aerosol vertical profiles: Anthropogenic impacts on optical depth and cloud nuclei. *Science* 329: 1488.

Clement C.F., Ford I.J., Twohy C.H., Weinheimer A. & Campos T. 2002. Particle production in the outflow of a midlatitude storm. *J. Geophys. Res.* 107(D21): 4559.

Collins D.R., Flagan R.C. & Seinfeld J.H. 2002. Improved Inversion of Scanning DMA Data. *Aerosol Science and Technology* 36: 1–9.

Crippa P., Petäjä T., Korhonen H., El Afandi G.S. & Pryor S.C. 2012. Evidence of an elevated source of nucleation based on model simulations and data from the NIFTy experiment. *Atmos. Chem. Phys. Discuss.* 12: 11979–12021.

Crumeyrolle S., Manninen H.E., Sellegri K., Roberts G., Gomes L., Kulmala M., Weigel R., Laj P. & Schwarzenboeck A. 2010. New particle formation events measured on board the ATR-42 aircraft during the EUCAARI campaign. *Atmos. Chem. Phys.* 10: 6721–6735.

Dal Maso M., Kulmala M., Riipinen I., Wagner R., Hussein T., Aalto P.P. & Lehtinen K.E.J. 2005. Formation and growth of fresh atmospheric aerosols: eight years of aerosol size distribution data from SMEAR II, Hyytiälä, Finland. *Boreal Env. Res.* 10: 323–336.

Forster P., Ramaswamy V., Artaxo P., Berntsen T., Betts R., Fahey D.W., Haywood J., Lean J., Lowe D.C., Myhre G., Nganga J., Prinn R., Raga G., Schulz M. & Van Dorland R. 2007. Changes in Atmospheric Constituents and in Radiative Forcing. In: Solomon S., Qin D., Manning M., Chen Z., Marquis M., Averyt K.B., Tignor M. & Miller H.L. (eds.), *Climate change 2007: The Physical Science Basis*, Contribution of Working Group I to the Fourth Assessment Report of the Intergovernmental

Panel on Climate Change, Cambridge University Press, Cambridge, UK, and New York, NY, USA.

Hamburger T., McMeeking G., Minikin A., Birmili W., Dall'Osto M., O'Dowd C.D., Flentje H., Henzing B., Junninen H., Kristensson A., de Leeuw G., Stohl A., Burkhart J.F., Coe H., Krejci R. & Petzold A. 2011. Overview of the synoptic and pollution situation over Europe during the EUCAARI-LONGREX field campaign. *Atmos. Chem. Phys.* 11: 1065–1082.

Hari P. & Kulmala M. 2005. Station for Measuring Ecosystem–Atmosphere Relations (SMEAR II). *Boreal Env. Res.* 10: 315–322.

Heald C.L., Coe H., Jimenez J.L., Weber R.J., Bahreini R., Middlebrook A.M., Russell L.M., Jolleys M., Fu T.-M., Allan J.D., Bower K.N., Capes G., Crosier J., Morgan W.T., Robinson N.H., Williams P.I., Cubison M.J., DeCarlo P.F. & Dunlea E.J. 2011. Exploring the vertical profile of atmospheric organic aerosol: comparing 17 aircraft field campaigns with a global model. *Atmos. Chem. Phys.* 11: 12673–12696.

Hinds W.C. 1999. *Aerosol technology*. Wiley, New York, USA.

Hussein T., Junninen H., Tunved P., Kristensson A., Dal Maso M., Riipinen I., Aalto P.P., Hansson H.-C., Swietlicki E. & Kulmala M. 2009. Time span and spatial scale of regional new particle formation events over Finland and southern Sweden. *Atmos. Chem. Phys.* 9: 4699–4716.

Junkermann W. 2001. An ultralight aircraft as platform for research in the lower troposphere: system performance and first results from radiation transfer studies in stratiform aerosol layers and broken cloud conditions. *J. Ocean. Atmos. Techn.* 18: 934–946.

Junkermann W. 2005. The actinic UV-radiation budget during the ESCOMPTE campaign 2001: results of airborne measurements with the microlight research aircraft D-MIFU. *Atmos. Res.* 74: 461–475.

Kerminen V.-M., Petäjä T., Manninen H.E., Paasonen P., Nieminen T., Sipilä M., Junninen H., Ehn M., Gagné S., Laakso L., Riipinen I., Vehkamäki H., Kurtén T., Ortega I.K., Dal Maso M., Brus D., Hyvärinen A., Lihavainen H., Leppä J., Lehtinen K.E.J., Mirme A., Mirme S., Hõrrak U., Berndt T., Stratmann F., Birmili W., Wiedensohler A., Metzger A., Dommen J., Baltensperger U., Kiendler-Scharr A., Mentel T.F., Wildt J., Winkler P.M., Wagner P.E., Petzold A., Minikin A., Plass-Dülmer C., Pöschl U., Laaksonen A. & Kulmala M. 2010. Atmospheric nucleation: highlights of the EUCAARI project and future directions. *Atmos. Chem. Phys.* 10: 10829–10848.

Komppula M., Lihavainen H., Kerminen V.-M., Kulmala M. & Viisanen Y. 2005. Measurements of cloud droplet activation of aerosol particles at a clean subarctic background site. *J. Geophys. Res.* 110(D6), D06204, doi:10.1029/2004JD005200.

Kulmala M. & Kerminen V.-M. 2008. On the formation and growth of atmospheric nanoparticles. *Atmos. Res.* 90: 132–150.

Kulmala M., Vehkamäki H., Petäjä T., Dal Maso M., Lauri A., Kerminen V.-M., Birmili W. & McMurry P.H. 2004. Formation and growth rates of ultrafine atmospheric particles: a review of observations. *Journal of Aerosol Science* 35: 143–176.

Kulmala M., Hämeri K., Aalto P.P., Mäkelä J.M., Pirjola L., Douglas Nilsson E., Buzorius G., Rannik Ü., Dal Maso M., Seidl W., Hoffman T., Janson R., Hansson H.-C., Viisanen Y., Laaksonen A. & O'Dowd C.D. 2001. Overview of the international project on biogenic aerosol formation in the boreal forest (BIOFOR). *Tellus* 53B: 324–343.

Kulmala M., Asmi A., Lappalainen H.K., Baltensperger U., Brenguier J.-L., Facchini M.C., Hansson H.-C., Hov Ø., O'Dowd C.D., Pöschl U., Wiedensohler A., Boers R., Boucher O., de Leeuw G., Denier van der Gon H.A.C., Feichter J., Krejci R., Laj P., Lihavainen H., Lohmann U., McFiggans G., Mentel T., Pilinis C., Riipinen I., Schulz M., Stohl A., Swietlicki E., Vignati E., Alves C., Amann M., Ammann M., Arabas S., Artaxo P., Baars H., Beddows D.C.S., Bergström R., Beukes J.P., Bilde M., Burkhart J.F., Canonaco F., Clegg S.L., Coe H., Crumeyrolle S., D'Anna B., Decesari S., Gilardoni S., Fischer M., Fjaeraa A.M., Fountoukis C., George C., Gomes L., Halloran P., Hamburger T., Harrison R.M., Herrmann H., Hoffmann T., Hoose C., Hu M., Hyvärinen A., Hõrrak U., Iinuma Y., Iversen T., Josipovic M., Kanakidou M., Kiendler-Scharr A., Kirkevåg A., Kiss G., Klimont Z., Kolmonen P., Komppula M., Kristjánsson J.-E., Laakso L., Laaksonen A., Labonnote L., Lanz V.A., Lehtinen K.E.J., Rizzo L.V., Makkonen R., Manninen H.E., McMeeking G., Merikanto J., Minikin A., Mirme S., Morgan W.T., Nemitz E., O'Donnell D., Panwar T.S., Pawlowska H., Petzold A., Pienaar J.J., Pio C., Plass-Duelmer C., Prévôt A.S.H., Pryor S., Reddington C.L., Roberts G., Rosenfeld D., Schwarz J., Seland Ø., Sellegri K., Shen X.J., Shiraiwa M., Siebert H., Sierau B., Simpson D., Sun J.Y., Topping D., Tunved P., Vaattovaara P., Vakkari V., Veefkind J.P., Visschedijk A., Vuollekoski H., Vuolo R., Wehner B., Wildt J., Woodward S., Worsnop D.R., van Zadelhoff G.-J., Zardini A.A., Zhang K., van Zyl P.G., Kerminen V.-M., Carslaw K.S. & Pandis S.N. 2011. General overview: European Integrated project on Aerosol Cloud Climate and Air Quality interactions (EUCAARI) — integrating aerosol research from nano to global scales. *Atmos. Chem. Phys.* 11: 13061–13143.

Laakso L., Grönholm T., Kulmala L., Haapanala S., Hirsikko A., Lovejoy E.R., Kazil J., Kurtén T., Boy M., Nilsson E.D., Sogachev A., Riipinen I., Stratmann F. & Kulmala M. 2007. Hot-air balloon measurements of vertical variation of boundary layer new particle formation. *Boreal Env. Res.* 12: 279–294.

Mäkelä J.M., Aalto P.P., Jokinen V., Pohja T., Nissinen A., Palmroth S., Markkanen T., Seitsonen K., Lihavainen H. & Kulmala M. 1997. Observations of ultrafine aerosol particle formation and growth in boreal forest. *Geophys. Res. Lett.* 24: 1219–1222.

McNaughton C.S., Clarke A.D., Howell S.G., Pinkerton M., Anderson B., Thornhill L., Hudgins C., Winstead E., Dibb J.E., Scheuer E. & Maring H. 2007. Results from the DC-8 Inlet Characterization Experiment (DICE): Airborne versus surface sampling of mineral dust and sea salt aerosols. *Aerosol Science and Technology* 41:

136–159.

Merikanto J., Spracklen D.V., Mann G.W., Pickering S.J. & Carslaw K.S. 2009. Impact of nucleation on global CCN. *Atmos. Chem. Phys.* 9: 8601–8616.

Mirme A., Tamm E., Mordas G., Vana M., Uin J., Mirme S., Bernotas T., Laakso L., Hirsikko A. & Kulmala M. 2007. A wide-range multi-channel air ion spectrometer. *Boreal Env. Res.* 12: 247–264.

Mirme S., Mirme A., Minikin A., Petzold A., Hõrrak U., Kerminen V.-M. & Kulmala M. 2010. Atmospheric sub-3nm particles at high altitudes. *Atmos. Chem. Phys.* 10: 437–451.

Nel A., Xia T., Mädler L. & Li N. 2006. Toxic Potential of Materials at the Nanolevel. *Science* 311: 622–627.

Nilsson E.D., Paatero J. & Boy M. 2001a. Effects of air masses and synoptic weather on aerosol formation in the continental boundary layer. *Tellus* 53B: 462–478.

Nilsson E.D., Rannik Ü., Kulmala M., Buzorius G. & O'Dowd C.D. 2001b. Effects of the continental boundary layer evolution, convection, turbulence and entrainment on aerosol tormation. *Tellus* 53B: 441–461.

O'Dowd C.D., Yoon Y.J., Junkermann W., Aalto P.P., Kulmala M., Lihavainen H. & Viisanen Y. 2007. Airborne measurements of nucleation mode particles I: coastal nucleation and growth rates. *Atmos. Chem. Phys.* 7: 1491–1501.

O'Dowd C.D., Yoon Y.J., Junkermann W., Aalto P.P., Kulmala M., Lihavainen H. & Viisanen Y. 2009. Airborne measurements of nucleation mode particles II: boreal forest nucleation events. *Atmos. Chem. Phys.* 9: 937–944.

Pryor S.C., Spaulding A.M. & Barthelmie R.J. 2010. New particle formation in the Midwestern USA: Event characteristics, meteorological context and vertical profiles. *Atmos. Environ.* 44: 4413–4425.

Pryor S.C., Barthelmie R.J., Sørensen L.L., McGrath J.G., Hopke P. & Petäjä T. 2011. Spatial and vertical extent of nucleation events in the Midwestern USA: insights from the Nucleation In ForesTs (NIFTy) experiment. *Atmos. Chem. Phys.* 11: 1641–1657.

Schröder F. & Ström J. 1997. Aircraft measurements of sub micrometer aerosol particles (> 7 nm) in the midlatitude free troposphere and tropopause region. *Atmos. Res.* 44: 333–356.

Sogacheva L., Dal Maso M., Kerminen V.-M. & Kulmala M. 2005. Probability of nucleation events and aerosol particle concentration in different air mass types arriving at Hyytiälä, southern Finland, based on back trajectories analysis. *Boreal Env. Res.* 10: 479–491.

Stanier C., Khlystov A. & Pandis S.N. 2004. Nucleation events during the Pittsburgh Air Quality Study: description and relation to key meteorological, gas phase, and aerosol parameters. *Aerosol Science and Technology* 38(S1): 253–264.

Tammet H. 2006. Continuous scanning of the mobility and size distribution of charged clusters and nanometer particles in atmospheric air and the Balanced Scanning Mobility Analyzer BSMA. *Atmos. Res.* 82: 523–535.

Vaclavik Bräuner E., Forchhammer L., Møller P., Simonsen J., Glasius M., Wåhlin P., Raaschou-Nielsen O. & Loft S. 2007. Exposure to ultrafine particles from ambient air and oxidative stress-induced DNA damage. *Environ Health Perspect* 115: 1177–1182.

Vana M., Kulmala M., Dal Maso M., Hõrrak U. & Tamm E. 2004. Comparative study of nucleation mode aerosol particles and intermediate air ions formation events at three sites. *J. Geophys. Res.* 109: 1–10.

Virkkula A., Levula J., Pohja T., de Leeuw G., Schultz D., Clements C., Kukkonen J., Nikmo J., Sofiev M., Pirjola L., Kulmala L., Pumpanen J., Vesala T., Kieloaho A.-J., Aaltonen H., Pihlatie M., Häkkinen S., Manninen H.E., Junninen H., Nieminen T. & Kulmala M. 2011. Prescribed forest burning experiment in June 2009. *Report Series in Aerosol Science* 126: 402–407.

Wang S.C. & Flagan R.C. 1990. Scanning electrical mobility spectrometer. *Aerosol Science and Technology* 13: 230–240.

Weber R.J., Chen G., Davis D.D., Mauldin R.L.III, Tanner D.J., Eisele F.L., Clarke A.D., Thornton D.C. & Bandy A.R. 2001. Measurements of enhanced $H_2SO_4$ and 3–4 nm particles near a frontal cloud during the First Aerosol Characterization Experiment (ACE 1). *J. Geophys. Res.* 106(D20): 24107–24117.

Weber R.J., Lee S., Chen G., Wang B., Kapustin V., Moore K., Clarke A.D., Mauldin L., Koschiuch E., Cantrell C., Eisele F., Thornton D.C., Bandy A.R., Sachse G.W. & Fuelberg H.E. 2003. New particle formation in anthropogenic plumes advecting from Asia observed during TRACE-P. *J. Geophys. Res.* 108(D21), 8814, doi:10.1029/2002JD003112.

Wehner B., Siebert H., Stratmann F., Tuch T., Wiedensohler A., Petäjä T., Dal Maso M. & Kulmala M. 2007. Horizontal homogeneity and vertical extent of new particle formation events. *Tellus* 59B: 362–371.

Wehner B., Siebert H., Ansmann A., Ditas F., Seifert P., Stratmann F., Wiedensohler A., Apituley A., Shaw R.A., Manninen H.E. & Kulmala M. 2010. Observations of turbulence-induced new particle formation in the residual layer. *Atmos. Chem. Phys.* 10: 4319–4330.

Yli-Juuti T., Nieminen T., Hirsikko A., Aalto P.P., Asmi E., Hõrrak U., Manninen H.E., Patokoski J., Dal Maso M., Petäjä T., Rinne J., Kulmala M. & Riipinen I. 2011. Growth rates of nucleation mode particles in Hyytiälä during 2003–2009: variation with particle size, season, data analysis method and ambient conditions. *Atmos. Chem. Phys.* 11: 12865–12886.

Yue D.L., Hu M., Zhang R.Y., Wu Z.J., Su H., Wang Z.B., Peng J.F., He L.Y., Huang X.F., Gong Y.G. & Wiedensohler A. 2011. Potential contribution of new particle formation to cloud condensation nuclei in Beijing. *Atmos. Environ.* 45: 6070–6077.